Influence of pressure on fast picosecond relaxation in glass-forming materials

L. Hong,[1] B. Begen,[1] A. Kisliuk,[2,3] V. N. Novikov,[2,3,4] and A. P. Sokolov[2,3,*]
[1]*Department of Polymer Science, The University of Akron, Akron, Ohio 44325-3909, USA*
[2]*Chemical Science Division, Oak Ridge National Laboratory, Oak Ridge, Tennessee 37831-6197, USA*
[3]*Department of Chemistry, The University of Tennessee, Knoxville, Tennessee 37996, USA*
[4]*Institute of Automation and Electrometry, Russian Academy of Sciences, Novosibirsk 630090, Russia*
(Received 10 December 2009; revised manuscript received 16 February 2010; published 30 March 2010)

Understanding the microscopic mechanism of the fast dynamics (gigahertz-terahertz frequency range) in amorphous materials remains a challenge. Disordered systems usually exhibit two additional contributions in this frequency range in comparison to their crystalline counterparts: a low-frequency excess vibrations, the so-called boson peak, and the fast picosecond relaxation that appears as a quasielastic scattering (QES) in the light- and neutron-scattering spectra. The nature of both contributions remains a subject of active discussions. In particular, QES intensity varies significantly with temperature. These variations might be caused by pure thermal effect and/or by change in density. To separate these two contributions we performed detailed light (Raman and Brillouin) scattering studies of the fast dynamics at different experimental conditions: isothermal, isobaric, isokinetic, and isochoric. The analysis demonstrates that the volume contribution dominates the fast relaxation behavior in a liquid state while the thermal energy becomes more important in the glassy state. Moreover, the presented analysis of the light-scattering data reveals significant difference in sensitivity of the fast dynamics to pressure among seven glass-forming materials (van der Waals-bonding and hydrogen-bonding molecular systems and polymers) studied in this work. It appears that the fast dynamics in orthoterphenyl and glycerol depends on pressure (density) significantly weaker than in other materials. However, the earlier observed correlations between pressure-induced variations in the QES and boson peak intensities and between the boson peak frequency and intensity are confirmed for all the studied materials. The obtained experimental results are compared to predictions of different models.

DOI: 10.1103/PhysRevB.81.104207 PACS number(s): 61.43.Fs, 63.50.−x, 64.70.P−

I. INTRODUCTION

Simple Debye model for vibrational density of states $g(\nu)$ in solids is based on the assumption of a homogeneous elastic continuum and predicts that $g_{\mathrm{Deb}}(\nu) \propto \nu^2$, ν is the vibrational frequency. It usually describes well the low-frequency [gigahertz (GHz)-terahertz (THz)] acoustic region of vibrational density of states in crystals. However, all disordered materials exhibit strong deviations from the predictions of the Debye model.[1] Two extra contributions exist in this GHz-THz (picosecond time scale) region of the excitation spectra in disordered systems: (i) an anharmonic relaxationlike contribution that appears as a broad quasielastic scattering (QES) and (ii) a harmonic vibration contribution, which appears as a broad inelastic peak, the so-called boson peak, in light- and neutron-scattering spectra.[2–4] These two contributions are observed in spectra of all glass-forming and amorphous materials, and even in spectra of biological macromolecules such as proteins, DNA, and RNA.[5–8] They reflect peculiarity of the fast picosecond dynamics general for soft materials. Additional interest to the fast dynamics was stimulated by experimental observations that reveal correlations between the GHz-THz dynamics and steepness of the temperature variations in the main structural relaxation.[9–17] Thus, understanding the microscopic mechanisms underlying the fast dynamics might have significant implications for understanding the glass transition phenomenon and, more general, dynamics in soft materials.

Despite a few decades of studies, the microscopic nature of the fast relaxation remains a subject of active discussions. There are essentially five different approaches proposed to describe the fast relaxation. (i) The asymmetric double-well potentials model (ADWP) ascribes the fast relaxation to conformational jumps over relatively low-energy barriers in the asymmetric double-well potentials.[18] The model assumes distributions of both the barrier height and the asymmetry. (ii) The soft potential model (SPM) combines in a unified approach some realization of the double-well potentials, tunneling systems and the soft harmonic oscillators representing the excess vibrations at the boson peak.[19,20] These three types of low-energy excitations have a common basis: soft atomic potentials. (iii) In the framework of the mode-coupling theory (MCT),[17] the fast picosecond relaxation is a precursor for the main structural relaxation and presents a rattling of structural units in a cage formed by their neighbors. (iv) Some researchers connected the fast relaxation to the free volume in glass-forming systems.[21,22] Within this approach, a change in the QES intensity with temperature was ascribed to the change in the fraction of free volume in the material. (v) Fast relaxation has been also ascribed to vibrational anharmonicity[23–25] that increases with temperature.

In recent years, external pressure has been extensively used in studies of the glass transition phenomenon to separate the influence of density (free volume) and thermal energy on sharp slowing down of structural relaxation.[26–31] These studies analyzed the pressure sensitivity of the glass transition temperature T_g, dT_g/dP, and the ratio between isochoric and isobaric apparent activation energies, E_V/E_P. The latter characterizes the relative contributions of thermal energy and volume to the variation in the structural relaxation

time. In general, E_V/E_P is very high (close to 1) in hydrogen-bonding materials, is lower, but still above 0.5 in most of polymers and is rather low (~0.5 and below) in most of the van der Waals liquids.[27] Moreover, the hydrogen-bonding systems also exhibit relatively low values of dT_g/dP.[27] The common explanation is that breaking of hydrogen bonds (i.e., purely energetic factor) controls the structural relaxation and change in volume plays only secondary role in these systems.

The roles of density and pure thermal energy in the fast dynamics remain essentially unexplored. A few recent papers reported the influence of pressure on the boson peak.[32–37] The studies revealed that the peak frequency ν_{BP} increases and its amplitude I_{BP} decreases with pressure while spectral shape of the peak remains unchanged.[32–37] Moreover, pressure-induced variations in $1/\nu_{BP}$ were found to be proportional to that of I_{BP} in several polymers.[36,37] Influence of pressure on the fast relaxation is even less studied.[15,38–41] The recent letter[15] reported a strong decrease in the QES intensity under pressure and emphasized a relationship between pressure-induced variations in the QES intensity (I_{QES}) and of the boson peak amplitude in a few glasses.[15] None of these studies addressed the role of density and thermal energy in influencing the fast relaxation, the question crucial for most of the models proposed for description of the fast dynamics in glass-forming systems.

This question is the focus of the present paper. It presents detailed light-scattering studies of variations in fast dynamics at various thermodynamic conditions: isobaric, isothermal, isochoric, and isokinetic (along T_g). The analysis reveals that volume variations dominate behavior of the fast relaxation above T_g while the thermal energy becomes the dominating factor in a glassy state. Moreover, presented comparison of light-scattering results for various materials (polymers, oligomers, van der Waals bonding, and hydrogen-bonding molecular systems) reveals significant difference in sensitivity of the fast dynamics to pressure. Glycerol and OTP exhibit much weaker pressure-induced variations in the fast dynamics than other studied materials. Despite this difference, the data for all the materials confirm the earlier found correlations between pressure-induced variations in the QES and boson peak intensities[15] and between the boson peak frequency and intensity.[36,37] The obtained experimental results are compared to predictions of different theoretical models.

II. EXPERIMENTAL

All the materials used in our studies were purchased from commercial sources: polyisoprene (PIP) with M_w =2450 g/mol and M_n=2410 g/mol (T_g=201 K,[42] Scientific Polymer); poly(methylphenyl siloxane) (PMPS) with M_w=25 600 g/mol and M_n=15 800 g/mol (T_g=247 K,[37] Polymer Source); oligomer of polystyrene (PS) with M_w =580 g/mol and M_n=540 g/mol (T_g=255 K,[15] Scientific Polymer); polyisobutylene (PIB) with M_w=3580 g/mol and M_n=3290 g/mol (T_g=195 K,[37] Polymer Standard Service); cumene (T_g=126 K,[43] Sigma-Aldrich); orthoterphenyl (OTP) (T_g=246 K,[15] Sigma-Aldrich); and glycerol (T_g =185 K,[15] Sigma-Aldrich). The samples were placed in a commercial anvil pressure cell (from D'Anvils), which can achieve pressure higher than 2 GPa. The pressure in the anvil cell was changed at room temperature and then the cell was mounted into optical cryofurnace to be cooled down or heated up to a desired temperature for further light-scattering measurement. The detailed description of the experimental procedure, including estimates of the pressure inside the cell, is presented in our earlier publication.[37]

The light-scattering spectra were measured in a 90° symmetric geometry, which has the advantage to compensate the refractive index and excludes influence of its pressure variations on the final results.[44] Solid-state laser (Verdi-2 from Coherent) with the wavelength 532 nm and power on the sample ~50–150 mW was used for the light-scattering measurements. Brillouin scattering spectra were measured using a tandem Fabry-Perot interferometer (Sandercock model) with two different free spectral ranges, 50 and 375 GHz. Longitudinal Brillouin modes were measured in polarized spectra. Depolarized scattering spectra were used to measure transverse-acoustic modes and the quasielastic-scattering spectra. The Raman spectra were measured using a Jobin Yvon T64000 triple monochromator in a subtractive mode. The polarized Raman spectra were used to estimate the sample temperature from the ratio of the Stokes and anti-Stokes intensities. Depolarized Raman spectra down to frequency ~200 GHz (good overlap with the interferometer data) were used to analyze the boson peak spectra. The intensity of the combined (Raman plus interferometer) depolarized scattering spectra were normalized at high-frequency optical modes in the range ~4–11 THz. This normalization provides intensity per mole of the sample.

III. ANALYSIS OF THE SPECTRA

The measured spectra were analyzed in the spectral density presentation, $I_n(\nu)=I(\nu)/\{\nu[n(\nu)+1]\}$, here $I(\nu)$ is the measured intensity and $[n(\nu)+1]$ is the Bose temperature factor. The spectra were fit by the traditional expression[45]

$$I_n(\nu) = \frac{A\nu_0}{\nu_0^2+\nu^2} + I_{BP}\exp\left\{-\frac{[\ln(\nu/\nu_{BP})]^2}{2W_0^2}\right\}, \qquad (1)$$

where the first term describes the quasielastic contribution presented by a Lorentzian function with width ν_0 and amplitude A, and the second term describes the boson peak approximated by a log-normal function with a width W_0. The typical spectra and detailed description of the data analysis have been presented in Refs. 15 and 37. Statistics of the QES part of the spectra (below 200 GHz) is not as good as in the boson peak region. For accurate analysis of the I_{QES}, we integrate the spectra in a certain frequency range. The so-obtained I_{QES} reduces the statistical error. For most of the materials studied here, the integration frequency range is from 100 to 200 GHz but it was from 250 to 350 GHz for glycerol and from 200 to 300 GHz for PIB. These two materials are weak light scatterers and only Raman data are available. At the same time, relatively high ν_{BP} in these two materials[15,37] allows analysis of the QES spectra at higher frequency.

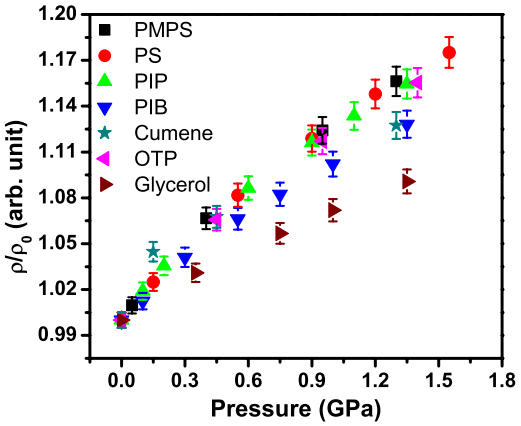

FIG. 1. (Color online) Pressure-induced variations in density at 140 K, except cumene (100 K), calculated for all the studied materials using Brillouin scattering data; ρ_0 is the density at ambient pressure.

The Brillouin peaks at different pressures were fitted by a simple Lorentzian function to estimate the frequency of the longitudinal ν_{LA} and transverse ν_{TA} Brillouin modes. These frequencies were used to calculate the corresponding sound velocity, V_{LA} and V_{TA}, using expression for the symmetric scattering geometry measured at $\theta=90°$,[37]

$$V_x = \frac{\lambda \nu_x}{2 \sin\frac{\theta}{2}} = \frac{\lambda \nu_x}{\sqrt{2}}; \quad x = \mathrm{TA,LA}. \tag{2}$$

Here λ is the wavelength of the laser light.

IV. DISCUSSION

A. Estimates of variations in density

The calculated sound velocities at different pressures were used to estimate the density variations in the samples under compression. The detailed procedures can be found in Refs. 37 and 46. Figure 1 shows the pressure-induced density variations for all the samples at constant temperature in a glassy state. Materials are compressed by 9–17 %, when applying pressure up to 1.5 GPa. Glycerol exhibits the smallest density variations. Its structural relaxation is also the least sensitive to pressure (among the materials studied here), as evidenced by its smallest value of dT_g/dP (Table I). However, compressibility and dT_g/dP are not directly related. For example, cumene and PIB have very similar pressure-induced density variations (Fig. 1) while their dT_g/dP differ significantly (Table I). Also PIP has higher compressibility in comparison to PIB (Fig. 1) but lower dT_g/dP (Table I). Moreover, variation in density in glycerol is only 30–40 % smaller than in other studied materials (Fig. 1) while its dT_g/dP is two to six times lower. In other words, glycerol has also the smallest $dT_g/d\rho$, i.e., the weakest sensitivity of the structural relaxation to volume. This property of glycerol is apparently caused by its hydrogen-bonded structure.

B. QES of PIP at different thermodynamic conditions

We chose PIP for detailed studies of the fast dynamics in various thermodynamic (isobaric, isochoric, isothermal, and isokinetic) conditions. For this purpose, we first established a PVT diagram (Fig. 2) using the estimated density of the sample at different P and T. Our PVT diagram at lower pressures is consistent with literature data[50] (Fig. 2). Based on the literature values for $T_g(P)$ in PIP,[42] we marked the isokinetic density in Fig. 2. In contrast to the isofree volume idea,[51] density at T_g in PIP clearly increases with pressure.

Figures 3 and 4 present the spectra of PIP at different experimental conditions: isothermal [Fig. 3(a)], isobaric [Fig. 3(b)], isokinetic [Fig. 3(c)], and isochoric (Fig. 4). The variation in I_{QES} in isothermal and isobaric conditions is much larger than the other two. Analysis of the integrated I_{QES} versus density for these conditions (Fig. 5) reveals a few interesting observations. First of all, the isothermal variations (solid line) are always weaker than the isobaric ones (dashed line). This result emphasizes that both, density and thermal energy, influence QES intensity and higher temperature leads to stronger I_{QES} at the same density. This result is consistent

TABLE I. Parameters of the studied systems: T_g is the glass transition temperature, m is the fragility parameter, E_V and E_P are isochoric and isobaric apparent activation energy for the structural relaxation.

	T_g (K)	dT_g/dP (K/GPa)	m	dm/dP (GPa^{-1})	E_V/E_P
PMPS	247[a]	280[b]	100[c]	0[b]	0.52[b]
PS	253[d]	260[d]	72[d]	−60[d]	0.52[e]
PIP	201[f]	178[b]	62[c]	−40[d]	0.76[b]
PIB	195[a]	240[b]	46[c]	… [g]	0.74[b]
Cumene	126[h]	86[h]	93[h]	−60[h]	0.63[h]
OTP	246[d]	260[b]	81[c]	0[i]	0.55[b]
Glycerol	185[d]	40[b]	53[c]	+35[b]	0.94[b]

[a]Reference 37.
[b]Reference 27.
[c]Reference 47.
[d]Reference 15.
[e]Reference 48.
[f]Reference 42.
[g]Not available.
[h]Reference 43.
[i]Reference 49.

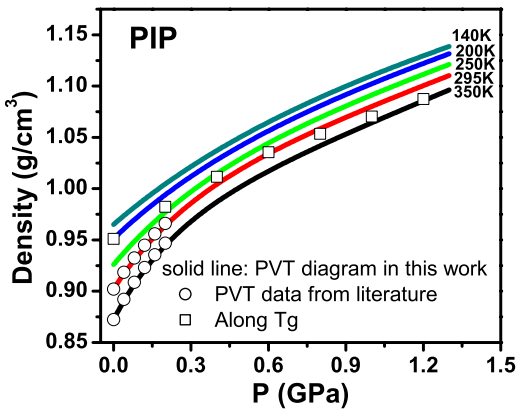

FIG. 2. (Color online) PVT diagram of PIP, the temperatures for each isothermal line are 140, 200, 250, 295, and 350 K from top to bottom. Empty circles are the PVT data from literature (Ref. 50). Empty squares indicate density along T_g (isokinetic).

with the earlier neutron-scattering data for OTP at the isochoric condition.[40] The difference between the isothermal and isobaric conditions is not significant above T_g but drastically increases below T_g. In other words, at a given density, the

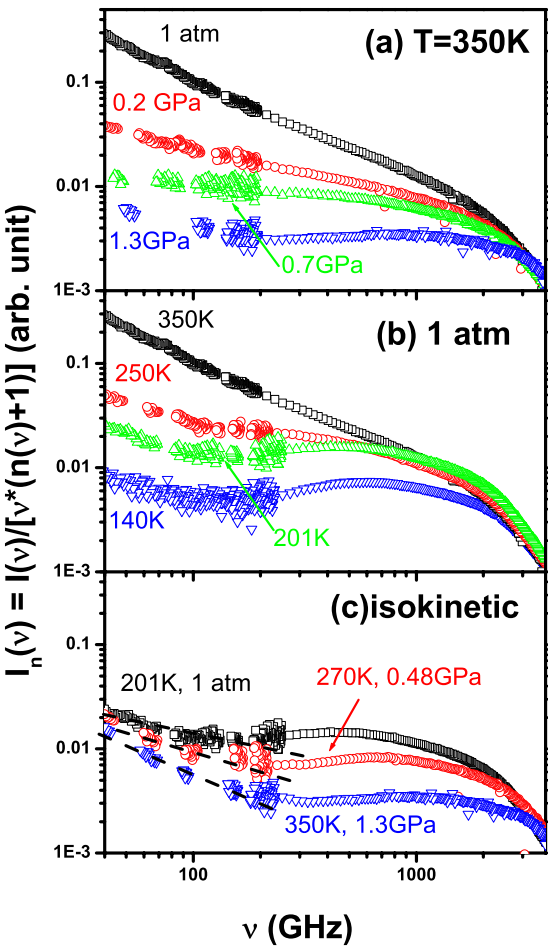

FIG. 3. (Color online) (a) Isothermal, (b) isobaric, and (c) isokinetic spectra of PIP. The dash lines in (c) present fit by a power law and show the slope of the QES spectra. 1 atm denotes the ambient pressure.

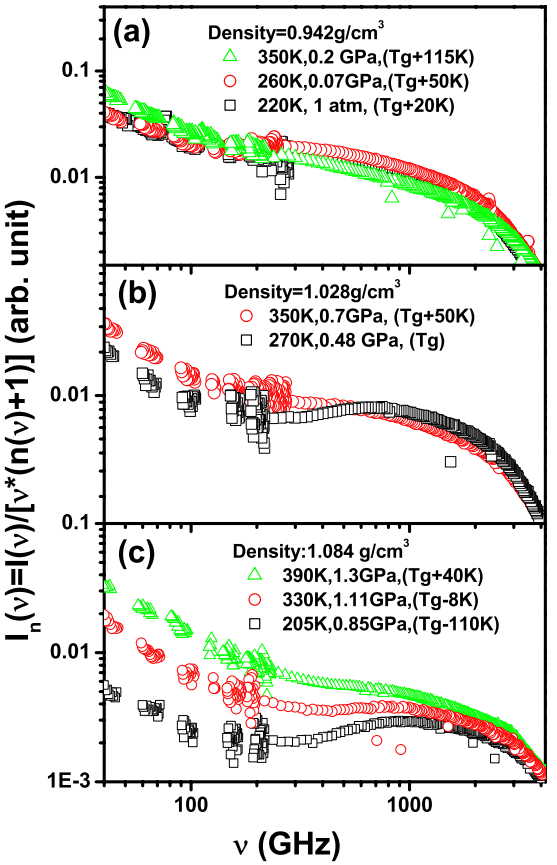

FIG. 4. (Color online) Isochoric spectra of PIP at three different densities: (a) 0.942 g/cm^3, (b) 1.028 g/cm^3, and (c) 1.084 g/cm^3.

thermal energy has minor influence on I_{QES} in a liquid state (above T_g) but it becomes dominating in a glassy state (below T_g). This conclusion is better illustrated using the ratio of the I_{QES} measured at the same density in the isobaric and in the isothermal conditions, $I_{QES}(P=1\ \text{atm})/I_{QES}(T=350\ \text{K})$ (inset Fig. 5). The ratio is essentially constant ($\sim$0.8) above T_g, emphasizing that the density variation is the dominating factor while it drops down significantly below T_g, where the pure thermal effects play the dominant role. This observation suggests that there is no direct relationship between QES intensity and density (free volume).

Second, the two isochoric measurements at temperatures above T_g and lower densities [Figs. 4(a) and 4(b), or isochoric 1 and isochoric 2 in Fig. 5] show no significant variations in the QES intensity, indicating again that density is the dominating variable above T_g. However, once the isochoric measurement crosses T_g [Fig. 4(c) or isochoric 3, i.e., Points A–C in Fig. 5], I_{QES} exhibits significant isochoric variations. In Fig. 5, points B and C are both below T_g, where, as we discussed above, thermal energy became important and that might be the main reason why these two points have so low I_{QES} in comparison to point A. Moreover, we want to stress that point A has been measured at $T=390$ K, i.e., outside of the established PVT diagram (was limited to $T=350$ K, Fig. 2). So, the density estimate at point A is not very accurate (and has large error bars). In addition, isochoric 3 covers the largest pressure variations (about 0.5 GPa), which also might be the reason for the significant variations in the QES intensity at constant volume.

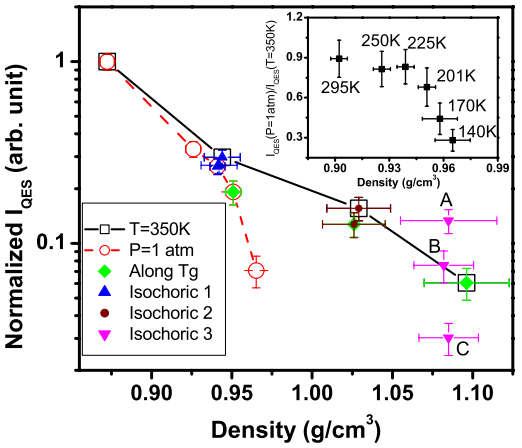

FIG. 5. (Color online) Integrated (from 100 to 200 GHz) QES intensity vs density in PIP for different thermodynamic conditions. It is normalized by the value at $T=350$ K and $P=1$ atm. The solid line with empty square (□) presents the isothermal condition ($T=350$ K); the dashed line with empty circle (○) presents the isobaric condition (ambient P); ♦ presents isokinetic conditions (along T_g); and ▲, ●, and ▼ present three isochoric cases. The inset presents the ratio between points along the dashed and the solid lines at the same density and the numbers denote the temperature along the dashed line.

Third, I_{QES} decreases with pressure in the isokinetic conditions (Fig. 5). At the same time, the spectral shape of the QES at T_g also varies with pressure [Fig. 3(c)]. These variations in the QES along the T_g line illustrate that the spectra of the fast relaxation measured at the same structural relaxation time might differ significantly. This behavior is different from the one known for the spectrum of the structural relaxation.[52,53] It agrees, however, with the earlier analysis of the depolarized light-scattering spectra of OTP above T_g.[41]

C. Pressure-induced variations in QES in different materials

As illustrated in Fig. 6, the pressure-induced variations in all the parameters (ν_{BP}, I_{BP}, and I_{QES}) in glycerol and OTP are significantly weaker than in other materials. This difference is intriguing and cannot be ascribed to a difference in intermolecular forces (glycerol is a hydrogen-bonding system, but OTP is a van der Waals bonding material, the same as cumene) or to the difference between polymers and small molecules (cumene and short PS exhibit the same behavior as polymers). Although glycerol has the weakest density change under pressure, variations in density in OTP is similar to the other studied materials (Fig. 1). Thus, sensitivity of density to pressure also cannot be the origin of the observed difference, as well as T_g, dT_g/dP, fragility m, i.e., the steepness of the temperature variations in the structural relaxation time at T close to T_g (Ref. 9) and its sensitivity to pressure dm/dP (Table I).

There is another interesting parameter, the length scale of the intermediate range order (or dynamic heterogeneity) ξ, which is often associated with the boson peak vibrations.[54–64] In the model of Schirmacher *et al.*,[58,59] ξ is

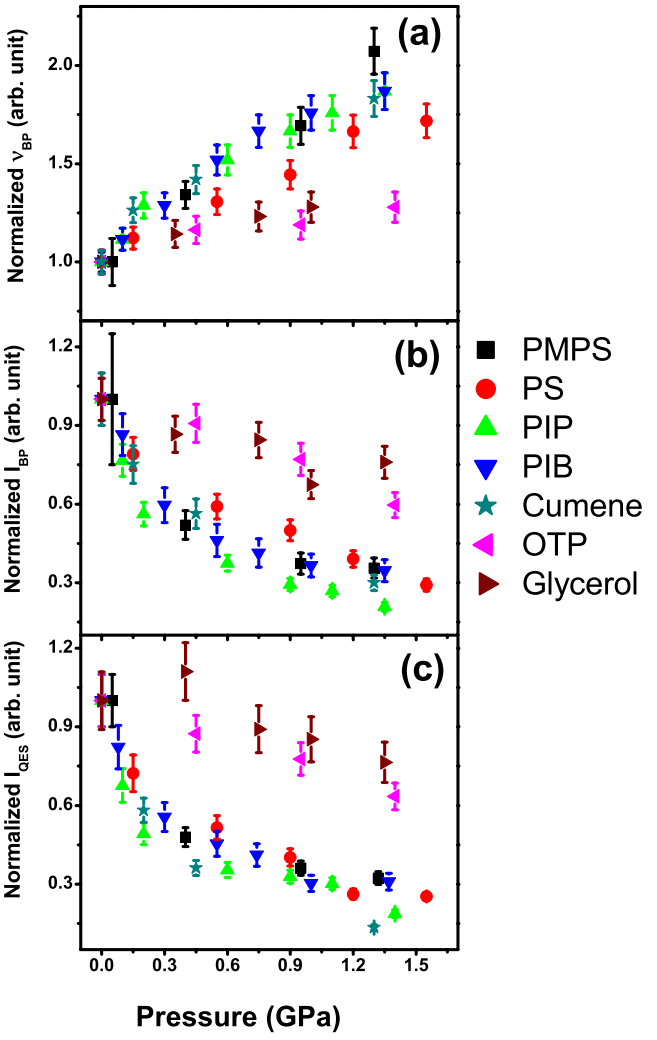

FIG. 6. (Color online) Pressure variations in (a) the boson peak frequency, (b) the boson peak amplitude, and (c) the QES intensity at $T=140$ K (except cumene where $T=100$ K). The values are normalized by the values at ambient pressure (except PMPS, where data are normalized by the value at $P=0.05$ GPa).

specified as a characteristic correlation length of elastic constants fluctuations. The simulation studies by Barrat *et al.* and Silbert *et al.* ascribe ξ to a length scale below which homogeneous elastic continuum approximation for deformation breaks down and structural heterogeneity becomes important.[60–63] Regardless of the particular model, ξ can be estimated from the frequency of the boson peak,[10,54,56–58,64,65]

$$\xi \approx S\frac{V_{TA}}{\nu_{BP}}. \tag{3}$$

Here the transverse sound velocity is used because the boson peak vibrations have mostly transverselike nature,[10,54,65] S is a constant ~0.5–1, depending on the model.[10,54,56–58,61,64–66] For simplicity, we assume that S does not vary significantly with pressure for all the samples.

Our analysis (Fig. 7) shows that ξ decreases significantly with pressure in most of the studied materials, in agreement

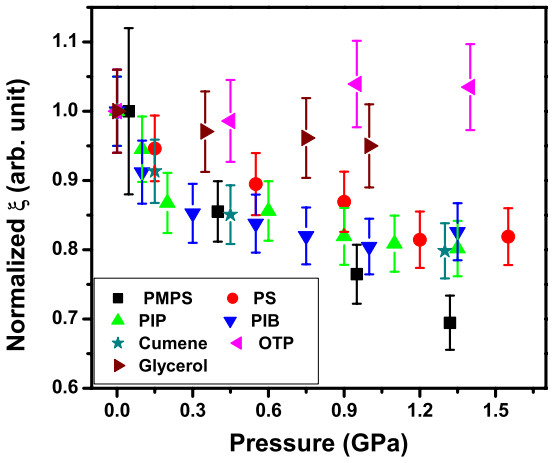

FIG. 7. (Color online) Pressure-induced variations in the correlation length ξ. The values of ξ are scaled by the values at ambient pressure (except PMPS, for which ξ is scaled by the value at $P=0.05$ GPa).

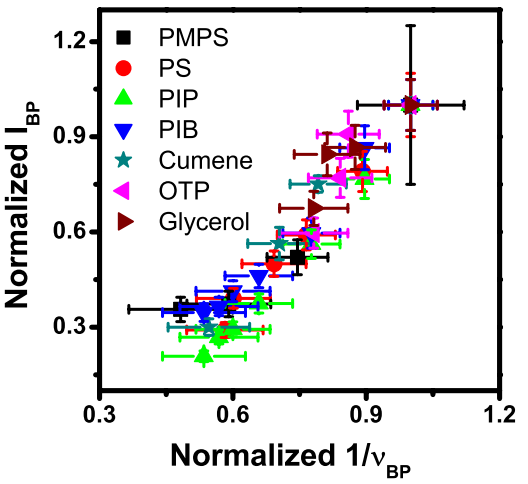

FIG. 8. (Color online) The boson peak amplitude vs inverse boson peak frequency, all the values are scaled by the values at ambient pressure except PMPS, for which the data are scaled by the value at $P=0.05$ GPa [the data are taken from Figs. 6(a) and 6(b)].

with our earlier studies of the boson peak[37] in a few polymers and the result of computer simulations.[62,63] But ξ does not vary much with pressure in glycerol and OTP (Fig. 7). This observation suggests that the systems where the characteristic heterogeneity length scale ξ is insensitive to densification also exhibit weak variations in the fast dynamics under pressure. So, there might be a direct connection between variations in the structure at the intermediate length scale and variations in the fast dynamics.

Despite significant difference in the sensitivity of the fast dynamics to pressure (Fig. 6), all the materials studied here follow two general trends reported earlier:[15,36,37] (i) the pressure-induced variations in I_{BP} correlate with that of $1/\nu_{\mathrm{BP}}$ (Fig. 8) and (ii) the change in I_{QES} with pressure correlates with that of I_{BP} (Fig. 9). It is surprising that the data for so diverse materials fall approximately on the same curves (Figs. 8 and 9). In another words, data points in Figs. 8 and 9 exhibit much smaller dependence on the material than in Figs. 6 and 7. This comparison indicates that the observations presented in Figs. 8 and 9 might be common features of the fast dynamics in all glass-forming materials regardless of their chemical structure.

Now we turn to analysis of the spectral shape of the QES. The susceptibility spectra of the fast relaxation usually exhibit a power-law behavior,[17,18,67–69]

$$\chi''(\nu) \propto I_n(\nu) \times \nu \propto \nu^{\alpha} \tag{4}$$

with the exponent $\alpha<1$. Our recent publication demonstrated that α decreases with pressure in three materials (PS, OTP, and PIP) at isothermal conditions.[15] In other words, the slope of the QES spectra presented as a spectral density became steeper under compression. Analysis of cumene and PMPS data (Fig. 10) reveals the same behavior. Moreover, our results show the decrease in the exponent α with pressure also for the isokinetic conditions (along T_g) in PIP [Fig. 3(c)] and cumene [Fig. 10(a)]. To provide a quantitative analysis of these variations, we fit the QES spectra to Eq. (4). The pressure dependence of the exponent α is different in different materials and conditions (isothermal or isokinetic) but it always decreases with pressure (Fig. 11).

V. COMPARISON OF EXPERIMENTAL DATA TO THEORETICAL MODELS

A. Indirect mechanism of the quasielastic scattering

Already in 1975, Winterling proposed two possible mechanisms of the QES contribution:[2] (i) a direct scattering on relaxation motions and (ii) an indirect mechanism of scattering on boson peak vibrations that are damped by some relaxation (similar to a Mountain mode in Brillouin scattering). According to this approach, the response function of a vibrational mode with a frequency Ω can be written as[2,4,70]

$$D(\Omega,\nu) = -\{\nu^2 - \Omega^2[1 - M(\nu)]\}^{-1}. \tag{5}$$

Here ν is the response frequency and $M(\nu)$ is a memory function that characterizes all processes damping the vibra-

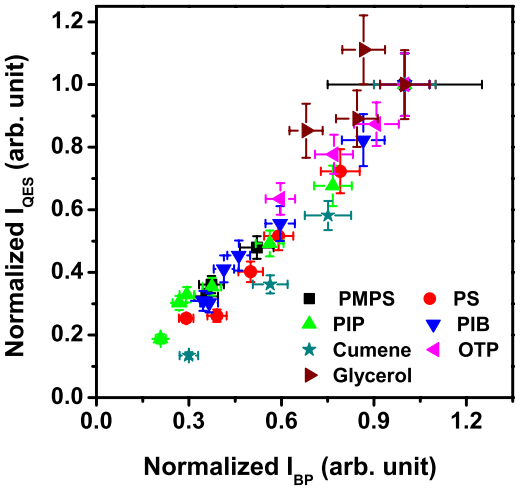

FIG. 9. (Color online) QES intensity vs boson peak amplitude (both scaled by the values at ambient pressure except PMPS, where data are normalized by the value at $P=0.05$ GPa. All the data are taken from Figs. 6(b) and 6(c) in isothermal condition.

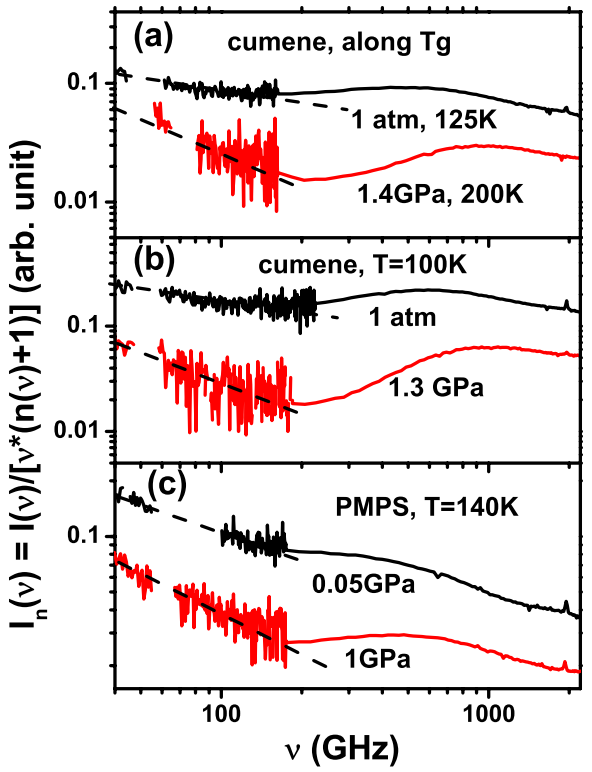

FIG. 10. (Color online) Pressure dependence of QES spectral shape: (a) cumene along T_g; (b) cumene at $T=100$ K; and (c) PMPS at $T=140$ K. The dash lines are fits by a power law to show the slope of the QES spectra.

tional mode. In that case, the susceptibility function of this mode, $\chi''(\Omega,\nu) \propto \mathrm{Im}[D(\Omega,\nu)]$, will have two contributions:[2,4,70] (i) an inelastic one at $\nu \sim \Omega[1-M'(\nu)]^{1/2}$ and (ii) a quasielastic one with the spectrum (at $\nu \ll \Omega$) $\chi''_{\mathrm{QES}}(\nu) \propto M''(\nu)/\Omega^2$ [here $M'(\nu)$ and $M''(\nu)$ are the real and imaginary parts of the memory term]. Because many modes are contributing to the spectrum around the boson peak, one needs to integrate their responses. As a result, one can write for the QES part of the light-scattering spectra,[4,70]

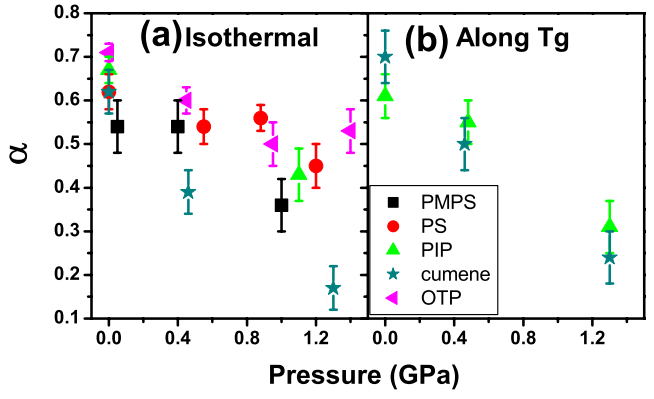

FIG. 11. (Color online) Pressure dependence of the slope α in (a) isothermal conditions at $T=140$ K (except cumene, $T=100$ K) and (b) isokinetic conditions (along T_g).

$$\chi''_{\mathrm{QES}}(\nu) = \frac{I_{ij}(\nu)}{n(\nu)+1} \approx M''(\nu)\int \frac{\chi''_{ij0}(\Omega)d\Omega}{\Omega\{[\nu^2/\Omega^2 - 1 + M'(\nu)]^2 + M''(\nu)^2\}}. \quad (6)$$

Here $I_{ij}(\nu)$ is the measured light-scattering spectrum with polarization ij, $\chi''_{ij0}(\Omega)$ is the vibrational spectrum without damping (e.g., at very low temperatures). Equation (6) emphasizes that the QES contribution has the spectral shape determined by the relaxation process $[M''(\nu)]$ but the QES properties (intensity, polarization, Q-dependence, etc.) are defined by the integrated properties of the vibrational modes, i.e., by the properties of the boson peak.[4,70]

Although the indirect mechanism did not receive much attention, there are several experimental evidences for a direct relationship between the boson peak and the QES contributions. For example, the depolarization ratio (the ratio of the depolarized to the polarized scattering intensities) for the QES contribution varies from ~0.25 for ZrF_4-BaF_2-LaF_3-AlF_3-NaF (ZBLAN) glass to ~0.75 in most of organic systems but in all cases it is the same as for the boson peak;[70] the wave-vector dependence of the QES contribution to the neutron-scattering spectra in SiO_2 and in polybutadiene (the only studied examples) appears to be the same as the Q-dependence of the boson peak vibrations.[70] More observations indicating the similarity of the QES properties to the properties of the boson peak have been summarized in Refs. 4 and 70. The observed correlation between the pressure-induced variations in the QES and of the boson peak intensities (Fig. 9) provides another evidence for the direct connection between these two contributions.

B. Pressure dependence of QES in soft potential model

The SPM describes excitations in glasses that are localized within effective potentials described by the fourth-order polynomial,[71]

$$U(x) = \varepsilon_0[\eta(x/a)^2 + \zeta(x/a)^3 + (x/a)^4]. \quad (7)$$

Here x is a generalized coordinate, a is the average interatomic distance, ε_0 is a characteristic atomic energy on the order of a few tenth electron volts. The parameters η and ζ vary from site to site. The distribution function $F(\eta,\zeta)$ of these parameters is an essential point of the model. It is assumed that this distribution is flat and proportional to the factor $|\eta|$ that accounts for the stability of the potential with respect to infinitesimal atomic displacements,

$$F(\eta,\zeta) = |\eta| P_0, \quad (8)$$

where P_0 is a constant. With different values of parameters the fourth-order polynomial potential can describe all kinds of asymmetric double-well potentials. In some region of the parameters the polynomial [Eq. (7)] describes a single-well potential with a small force constant and the corresponding excitations comprise the boson peak.

According to SPM, the low-frequency side of the boson peak is described by a power law,

$$I_{vib}(\nu) = \frac{g(\nu)}{\nu^2} = \frac{P_s}{24}\frac{\nu^2}{W^5} = A\nu^2, \tag{9}$$

and the relaxation contribution to the scattering signal is equal to[72,73]

$$I_{\mathrm{QES}}(\nu) = \frac{P_s}{2}\frac{T^{3/4}}{\nu W^{11/4}}. \tag{10}$$

Here P_s is the density of excess modes around the zero eigenvalue, calculated per atom, and W is the crossover energy between vibrational and tunneling states. P_s can vary with pressure and the detail dependence will be discussed later, whereas the pressure variations in W can be found using its relation with other SPM's parameters. Specifically,

$$W = \varepsilon_0 \eta_L^2, \tag{11}$$

where $\varepsilon_0 \sim m_0 V^2$ is a characteristic energy of the lattice, V is the sound velocity, and m_0 is the molecular mass. SPM does not distinguish longitudinal and transverse sound velocities. In our analysis, we tentatively use the transverse sound velocity because the boson peak vibrations have mostly transverselike nature.[10,54,65] The dimensionless parameter η_L is equal to

$$\eta_L = \left(\frac{\hbar^2}{2m_0 a^2 \varepsilon_0}\right)^{1/3}. \tag{12}$$

Thus, W can be expressed via experimentally measured sound velocity V and mass density $\rho \sim m_0/a^3$,

$$W = \varepsilon_0^{1/3}\left(\frac{\hbar^2}{2m_0 a^2}\right)^{2/3} = \mathrm{const} \times \rho^{4/9} V^{2/3}. \tag{13}$$

Analysis of the boson peak in glasses under pressure within the framework of SPM was presented in Ref. 74. According to the model, the boson peak spectrum has two universal regimes for the excess density of vibrational states (eDOS): $g_1(\nu) = A\nu^4$ at $\nu < \nu_{\mathrm{BP}}$ and $g_2(\nu) = B\nu$ at $\nu > \nu_{\mathrm{BP}}$.[75] Three predictions were made in Refs. 74 and 75: (i) $\nu_{\mathrm{BP}}(P) = \nu_{\mathrm{BP}}(0)(1 + P/P_0)^{1/3}$; (ii) $A \propto 1/P$; and (iii) B is pressure independent. The relationship between variations in the boson peak position and amplitude under pressure was not discussed in Ref. 74 but it was revealed in the later work[36] that pressure-induced variations in the boson peak follow the relationship,

$$I_{\mathrm{BP}}(P)\nu_{\mathrm{BP}}(P) \approx \mathrm{const}. \tag{14}$$

Reference 36 only briefly referred to this point but here we will discuss it in more details. With two limiting regimes of eDOS mentioned above, the whole spectrum in the region of the boson peak can be well approximated by

$$\frac{1}{g(\nu)} = \frac{1}{g_1(\nu)} + \frac{1}{g_2(\nu)} = \frac{1}{A\nu^4} + \frac{1}{B\nu}. \tag{15}$$

Thus, the boson peak spectrum (i.e., excess vibrations) is represented by the expression

$$\frac{g(\nu)}{\nu^2} = \frac{A\nu^2}{1 + (A/B)\nu^3}. \tag{16}$$

From Eq. (16) one can find the position ν_{BP} and the amplitude I_{BP} of the boson peak,

$$\nu_{\mathrm{BP}} = \left(\frac{2B}{A}\right)^{1/3}, \tag{17}$$

$$I_{\mathrm{BP}} = \frac{2^{2/3}}{3} B^{2/3} A^{1/3}. \tag{18}$$

As a result,

$$I_{\mathrm{BP}}\nu_{\mathrm{BP}} = \frac{2}{3}B. \tag{19}$$

Since B does not depend on pressure, the product of $I_{\mathrm{BP}}\nu_{\mathrm{BP}}$ should be pressure invariant. This prediction is consistent with the neutron-scattering data of PIB (Ref. 36) and provides a qualitative explanation to the general correlation between I_{BP} and $1/\nu_{\mathrm{BP}}$ in the light-scattering spectra of the materials studied here (Fig. 8).

Combining Eqs. (9), (13), and (18), the value of P_s can be derived as

$$P_s = \mathrm{const} \times \frac{I_{\mathrm{BP}}}{\nu_{\mathrm{BP}}^2} \times W^5 = \mathrm{const} \times \frac{I_{\mathrm{BP}}}{\nu_{\mathrm{BP}}^2} \times \rho^{20/9} V^{10/3}. \tag{20}$$

Unfortunately, the explicit pressure dependence of P_s cannot be obtained from analysis of the light-scattering data because the obtained I_{BP} involves the light-to-vibration coupling coefficient, which is known to be pressure dependent.[35] To study the pressure variations in P_s, we use the neutron-scattering data, which measure vibrational $g(\nu)$ directly. Analysis of earlier neutron-scattering data[36] demonstrates that P_s in PIB decreases under pressure by $\sim$40% at $P \sim 1.4$ GPa [Fig. 12(a)].

Combining Eqs. (9), (10), (13), and (18), the ratio of the intensity of the fast relaxation to that of the boson peak can be expressed as

$$\frac{I_{\mathrm{QES}}}{I_{\mathrm{BP}}} \propto \frac{P_s^{2/3} T^{3/4}}{\nu B^{2/3} W^{13/12}} \propto \frac{P_s^{2/3}}{\rho^{13/27} V^{13/18}}. \tag{21}$$

Since the pressure variation in P_s is known in the case of PIB, we can compare the experimental data of $I_{\mathrm{QES}}/I_{\mathrm{BP}}$ with the prediction of Eq. (21): $I_{\mathrm{QES}}/I_{\mathrm{BP}}$ should always decrease with pressure because both the sound velocity and density of materials increase and P_s decreases under pressure. This prediction clearly fails for PIB [Fig. 12(b)]. Moreover, the experimental results show that the studied materials have diverse behavior [Fig. 12(b)]: $I_{\mathrm{QES}}/I_{\mathrm{BP}}$ decreases with pressure in the case of PS and cumene, remains constant for PIP, PIB, and PMPS, and even slightly increases for glycerol. This analysis suggests that SPM cannot explain the correlation between the pressure-induced variations in the boson peak and QES intensities (Fig. 9).

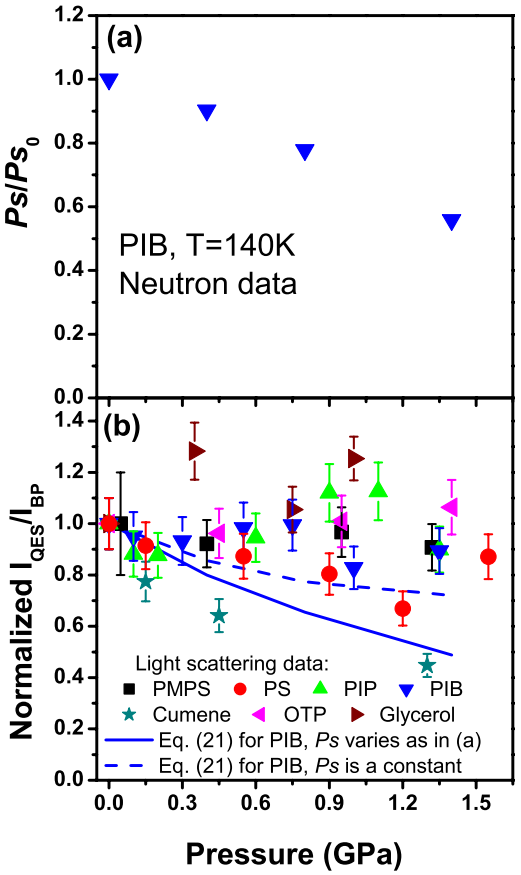

FIG. 12. (Color online) (a) Pressure dependence of the SPM parameter P_s in PIB normalized by the value at ambient P. Neutron-scattering data from Ref. 36 were used for these estimates. (b) Pressure variations in the ratio I_{QES}/I_{BP}: symbols—experimental data; solid line—the SPM prediction [Eq. (21)] for PIB assuming P_s varying with pressure as in (a); and dashed line—the same prediction for PIB assuming P_s is constant.

C. Spectral shape of the fast relaxation

The power-law spectrum [Eq. (4)] of the fast dynamics has been predicted by both the MCT (Ref. 17) and the ADWP model.[18] According to the MCT,[17] the exponent α should be a constant that depends on mode-mode coupling in the material while ADWP model predicts that α should increase linearly with temperature $\alpha \approx kT/E_0$ at $kT < E_0$, where E_0 is a characteristic energy barrier in a distribution of the barriers.[18] These ideas have been applied to analysis of the fast dynamics in several glass-forming systems and both temperature-dependent and temperature-independent behaviors of the exponent α have been observed.[67–69] However, the MCT predictions are valid in a high-temperature liquid and cannot be compared to our data measured mostly in a glassy state. The experimental data (Fig. 11) clearly demonstrate that the exponent α decreases under pressure. Within the framework of ADWP model, this observation suggests that densification of glass-forming materials leads to an increase in the characteristic activation energy barriers (E_0) for the fast relaxation. This effect is even stronger in the isokinetic conditions. For example, E_0 changes from 165 to 600 K in isothermal conditions ($T=140$ K) and it varies from 175 to 850 K in isokinetic case for cumene at pressures up to 1.4 GPa. Thus, compression in all the cases affects significantly potential-energy landscape and it seems that E_0 changes under pressure even stronger than T_g (Table I).

VI. CONCLUSIONS

We present detailed light-scattering studies of the fast dynamics under various thermodynamic conditions (isothermal, isobaric, isokinetic, and isochoric). The analysis reveals that density plays a dominant role in variation in the QES intensity above T_g (in a liquid state) while thermal energy (pure temperature effect) becomes the more important factor in the glassy state (below T_g). Our studies also demonstrate that sensitivity of the fast dynamics to pressure varies significantly among different materials with glycerol and OTP showing the weakest pressure-induced variations. These materials also have the smallest variations in the heterogeneity length scale defined as V_{TA}/ν_{BP}. Whether there is any correlation between pressure-induced variations in the medium-range structure and fast dynamics remains unclear. Despite this difference, the earlier reported correlations between the pressure-induced variations in the QES and boson peak intensities and the boson peak intensity and frequency were found to hold for all the materials studied here. We show that the first correlation can be explained assuming indirect mechanism of the quasielastic scattering and the second one agrees with the prediction of SPM.

ACKNOWLEDGMENTS

The authors acknowledge financial support by the NSF Polymer program (Grant No. DMR-0804571). A.K. acknowledges financial support by the Division of Materials Sciences and Engineering, DOE's BES. V.N.N. acknowledges the financial support from the Russian Foundation for Basic Research.

*Author to whom correspondence should be addressed; sokolov@utk.edu

[1] *Amorphous Solids: Low-Temperature Properties*, edited by W. A. Phillips (Springer-Verlag, Berlin, 1981).
[2] G. Winterling, Phys. Rev. B **12**, 2432 (1975).
[3] U. Buchenau, H. M. Zhou, N. Nucker, K. S. Gilroy, and W. A. Phillips, Phys. Rev. Lett. **60**, 1318 (1988).
[4] A. P. Sokolov, V. N. Novikov, and B. Strube, Europhys. Lett. **38**, 49 (1997).
[5] T. S. Grigera, V. Martin-Mayor, G. Parisi, and P. Verrocchio, Nature (London) **422**, 289 (2003).
[6] B. Frick and D. Richter, Science **267**, 1939 (1995).

[7] M. Ferrand, A. J. Dianoux, W. Petry, and G. Zaccai, Proc. Natl. Acad. Sci. U.S.A. **90**, 9668 (1993).
[8] Y. Joti, A. Kitao, and N. Go, J. Am. Chem. Soc. **127**, 8705 (2005).
[9] C. A. Angell, Science **267**, 1924 (1995).
[10] A. P. Sokolov, R. Calemczuk, B. Salce, A. Kisliuk, D. Quitmann, and E. Duval, Phys. Rev. Lett. **78**, 2405 (1997).
[11] L. E. Bove, C. Petrillo, A. Fontana, and A. P. Sokolov, J. Chem. Phys. **128**, 184502 (2008).
[12] A. P. Sokolov, E. Rossler, A. Kisliuk, and D. Quitmann, Phys. Rev. Lett. **71**, 2062 (1993).
[13] V. N. Novikov, Y. Ding, and A. P. Sokolov, Phys. Rev. E **71**, 061501 (2005).
[14] K. L. Ngai, A. Sokolov, and W. Steffen, J. Chem. Phys. **107**, 5268 (1997).
[15] L. Hong, B. Begen, A. Kisliuk, S. Pawlus, M. Paluch, and A. P. Sokolov, Phys. Rev. Lett. **102**, 145502 (2009).
[16] L. Larini, A. Ottochian, C. De Michele, and D. Leporini, Nat. Phys. **4**, 42 (2008).
[17] W. Gotze and L. Sjogren, Rep. Prog. Phys. **55**, 241 (1992).
[18] K. S. Gilroy and W. A. Phillips, Philos. Mag. B **43**, 735 (1981).
[19] V. G. Karpov, M. I. Klinger, and F. N. Ignatiev, Zh. Eksp. Teor. Fiz. **84**, 760 (1983).
[20] V. L. Gurevich, D. A. Parshin, J. Pelous, and H. R. Schober, Phys. Rev. B **48**, 16318 (1993).
[21] V. N. Novikov, A. P. Sokolov, B. Strube, N. V. Surovtsev, E. Duval, and A. Mermet, J. Chem. Phys. **107**, 1057 (1997).
[22] S. Kojima and V. N. Novikov, Phys. Rev. B **54**, 222 (1996).
[23] V. N. Novikov, Phys. Rev. B **58**, 8367 (1998).
[24] E. Rat, M. Foret, G. Massiera, R. Vialla, M. Arai, R. Vacher, and E. Courtens, Phys. Rev. B **72**, 214204 (2005).
[25] R. Vacher, E. Courtens, and M. Foret, Phys. Rev. B **72**, 214205 (2005).
[26] G. Floudas, C. Gravalides, T. Reisinger, and G. Wegner, J. Chem. Phys. **111**, 9847 (1999).
[27] C. M. Roland, S. Hensel-Bielowka, M. Paluch, and R. Casalini, Rep. Prog. Phys. **68**, 1405 (2005).
[28] C. Alba-Simionesco, D. Kivelson, and G. Tarjus, J. Chem. Phys. **116**, 5033 (2002).
[29] S. Hensel-Bielowka, S. Pawlus, C. M. Roland, J. Ziolo, and M. Paluch, Phys. Rev. E **69**, 050501(R) (2004).
[30] M. Paluch, C. M. Roland, and S. Pawlus, J. Chem. Phys. **116**, 10932 (2002).
[31] C. M. Roland, M. Paluch, T. Pakula, and R. Casalini, Philos. Mag. **84**, 1573 (2004).
[32] A. Monaco, A. I. Chumakov, G. Monaco, W. A. Crichton, A. Meyer, L. Comez, D. Fioretto, J. Korecki, and R. Ruffer, Phys. Rev. Lett. **97**, 135501 (2006).
[33] K. S. Andrikopoulos, D. Christofilos, G. A. Kourouklis, and S. N. Yannopoulos, J. Non-Cryst. Solids **352**, 4594 (2006).
[34] J. Schroeder, W. M. Wu, J. L. Apkarian, M. Lee, L. Hwa, and C. T. Moynihan, J. Non-Cryst. Solids **349**, 88 (2004).
[35] B. Begen, A. Kisliuk, V. N. Novikov, A. P. Sokolov, K. Niss, A. Chauty-Cailliaux, C. Alba-Siminoesco, and B. Frick, J. Non-Cryst. Solids **352**, 4583 (2006).
[36] K. Niss, B. Begen, B. Frick, J. Ollivier, A. Beraud, A. P. Sokolov, V. N. Novikov, and C. Alba-Simionesco, Phys. Rev. Lett. **99**, 055502 (2007).
[37] L. Hong, B. Begen, A. Kisliuk, C. Alba-Simionesco, V. N. Novikov, and A. P. Sokolov, Phys. Rev. B **78**, 134201 (2008).
[38] G. Li, H. E. King, Jr., W. F. Oliver, C. A. Herbst, and H. Z. Cummins, Phys. Rev. Lett. **74**, 2280 (1995).
[39] A. Tölle, H. Schober, J. Wuttke, O. G. Randl, and F. Fujara, Phys. Rev. Lett. **80**, 2374 (1998).
[40] A. Tölle, H. Schober, J. Wuttke, F. Fujara, and O. Randl, Physica B **234-236**, 428 (1997).
[41] A. Patkowski, M. Matos Lopes, and E. W. Fischer, J. Chem. Phys. **119**, 1579 (2003).
[42] E. N. Dalal and P. J. Phillips, Macromolecules **16**, 890 (1983).
[43] K. Niss, C. Dalle-Ferrier, V. M. Giordano, G. Monaco, B. Frick, and C. Alba-Simionesco, J. Chem. Phys. **129**, 194513 (2008).
[44] C. H. Whitfield, E. M. Brody, and W. A. Bassett, Rev. Sci. Instrum. **47**, 942 (1976).
[45] V. K. Malinovsky, V. N. Novikov, and A. P. Sokolov, Phys. Lett. A **153**, 63 (1991).
[46] J. M. Brown, L. J. Slutsky, K. A. Nelson, and L.-T. Cheng, Science **241**, 65 (1988).
[47] Q. Qin and G. B. Mckenna, J. Non-Cryst. Solids **352**, 2977 (2006).
[48] C. M. Roland, K. J. McGrath, and R. Casalini, J. Non-Cryst. Solids **352**, 4910 (2006).
[49] K. U. Schug, H. E. King, and R. Bohmer, J. Chem. Phys. **109**, 1472 (1998).
[50] C. M. Roland, M. Paluch, and R. Casalini, J. Polym. Sci., Part B: Polym. Phys. **42**, 4313 (2004).
[51] T. Fox and P. Flory, J. Appl. Phys. **21**, 581 (1950).
[52] C. M. Roland, R. Casalini, and M. Paluch, Chem. Phys. Lett. **367**, 259 (2003).
[53] K. L. Ngai, R. Casalini, S. Capaccioli, M. Paluch, and C. M. Roland, J. Phys. Chem. B **109**, 17356 (2005).
[54] S. R. Elliott, Europhys. Lett. **19**, 201 (1992).
[55] M. I. Klinger, Phys. Lett. A **170**, 222 (1992).
[56] D. Quitmann and M. Soltwisch, Philos. Mag. B **77**, 287 (1998).
[57] E. Duval, A. Boukenter, and T. Achibat, J. Phys.: Condens. Matter **2**, 10227 (1990).
[58] W. Schirmacher, B. Schmid, C. Tomaras, G. Viliani, G. Baldi, G. Ruocco, and T. Scopigno, Phys. Status Solidi C **5**, 862 (2008).
[59] B. Schmid and W. Schirmacher, Phys. Rev. Lett. **100**, 137402 (2008).
[60] F. Léonforte, A. Tanguy, J. P. Wittmer, and J.-L. Barrat, Phys. Rev. Lett. **97**, 055501 (2006).
[61] F. Leonforte, R. Boissiere, A. Tanguy, J. P. Wittmer, and J.-L. Barrat, Phys. Rev. B **72**, 224206 (2005).
[62] M. Wyart, L. E. Silbert, S. R. Nagel, and T. A. Witten, Phys. Rev. E **72**, 051306 (2005).
[63] L. E. Silbert, A. J. Liu, and S. R. Nagel, Phys. Rev. Lett. **95**, 098301 (2005).
[64] L. Hong, P. D. Gujrati, V. N. Novikov, and A. P. Sokolov, J. Chem. Phys. **131**, 194511 (2009).
[65] A. P. Sokolov, A. Kisliuk, M. Soltwisch, and D. Quitmann, Phys. Rev. Lett. **69**, 1540 (1992).
[66] V. Lubchenko and P. G. Wolynes, Annu. Rev. Phys. Chem. **58**, 235 (2007).
[67] S. V. Adichtchev, N. V. Surovtsev, J. Wiedersich, A. Brodin, V. N. Novikov, and E. A. Rössler, J. Non-Cryst. Solids **353**, 1491 (2007).
[68] J. Wiedersich, N. V. Surovtsev, V. N. Novikov, E. Rössler, and A. P. Sokolov, Phys. Rev. B **64**, 064207 (2001).
[69] N. V. Surovtsev, J. A. H. Wiedersich, V. N. Novikov, E. Rössler, and A. P. Sokolov, Phys. Rev. B **58**, 14888 (1998).

[70] A. P. Sokolov, V. N. Novikov, and B. Strube, Phys. Rev. B **56**, 5042 (1997).
[71] Y. M. Galperin, V. G. Karpov, and V. I. Kozub, Adv. Phys. **38**, 669 (1989).
[72] U. Buchenau, A. Wischnewski, M. Ohl, and E. Fabiani, J. Phys.: Condens. Matter **19**, 205106 (2007).
[73] B. Rufflé, D. A. Parshin, E. Courtens, and R. Vacher, Phys. Rev. Lett. **100**, 015501 (2008).
[74] V. L. Gurevich, D. A. Parshin, and H. R. Schober, Phys. Rev. B **71**, 014209 (2005).
[75] V. L. Gurevich, D. A. Parshin, and H. R. Schober, Phys. Rev. B **67**, 094203 (2003).